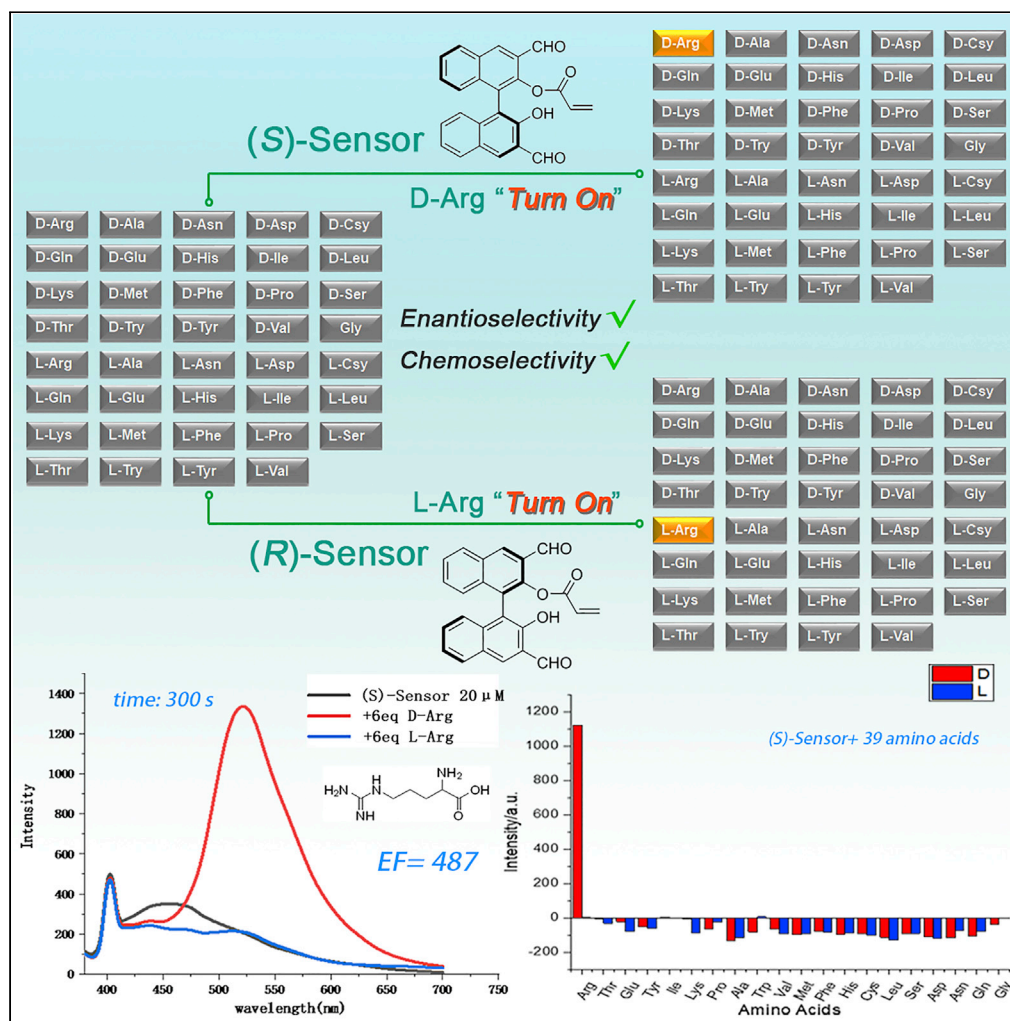## Article

Rapid, enantioselective and colorimetric detection of D-arginine

Xianzhe Yu, Binjie
Zhang, Cailing
Fan, ..., Gengyu
Du, Yanan Gao,
Chaoyuan Zeng

gd4eu@virginia.edu (G.D.)
ygao@hainanu.edu.cn (Y.G.)
zengchaoyuan@hainanu.edu.
cn (C.Z.)

Highlights

A new strategy to form a
fluorescent probe (S)-3
with multiple reaction
sites

Specific response to
D-arginine among 39
chiral amino acids

Metal-free detection,
quick responses within a
minute

Qualitative determination
of arginine through
colorimetric studies

iScience

Article

Rapid, enantioselective and colorimetric detection of D-arginine

Xianzhe Yu,[1,3] Binjie Zhang,[1,3] Cailing Fan,[1] Qianqian Yan,[1] Shenglin Wang,[1] Hui Hu,[1] Qinxi Dong,[1] Gengyu Du,[2,*] Yanan Gao,[1,*] and Chaoyuan Zeng[1,4,*]

SUMMARY

D-amino acids are of biological significance yet are not clearly understood due to the lack of powerful analytical tools for their identification. Thus, the specific detection of a single enantiomer of a particular amino acid remains a great challenge due to their structural similarity. Here, we report a strategy to incorporate multiple reaction sites on a chiral 1,1′-bi-2,2′-naphthol-based fluorescent probe. It can respond specifically to D-arginine, while producing no response when in contact with all other amino acids. The probe can report arginine's concentration, and enantiomeric configuration and colorimetric studies enable its qualitative determination.

INTRODUCTION

While L-amino acids have been found particularly important in many biofunctions (Maze et al., 2014; Lemos et al., 2019; Murray, 2016; Chen et al., 2018), recent studies have discovered that the uncommon D-amino acids also play important roles in biological systems, such as in memory and growth (Sievers et al., 2011; Sasabe et al., 2016; Garton et al., 2018; Dai et al., 2019; Beltrán-Castillo et al., 2017; Henneberger et al., 2010). So far, D-serine (Ser) is found to be an indicator for early-stage tumor growth and to be important as a human neurotransmitter. An abnormality in levels of D-serine will eventually lead to schizophrenia, amyotrophic lateral sclerosis, Alzheimer's disease or Parkinson's disease (Balu et al., 2013, 2014; Neame et al., 2019). D-aspartic acid (D-Asp) can promote the release of prolactin and regulate the concentration of melatonin, and poor D-Asp availability may cause sexual dysfunction (D'Aniello, 2007), while D-arginine (D-Arg) displays higher potency and broader toxicity in terms of the number of bacterial species affected (Chen et al., 2021; Shmueli et al., 2019; Alvarez et al., 2018). However, the understanding of the biofunction of D-amino acids remains unclear and incomplete, mostly due to technical limitations of their detection. Thus, developing strategies to detect D-amino acids is crucial. The differentiation between D- and L-amino acids is challenging as they are related only enantiomers and so asymmetric tools must be established. Furthermore, specific detection of a particular enantiomer of a single amino acid is even more difficult due to their structural similarities.

The enantioselective detection of free amino acids has always been challenging. 1,1′-Bi-2,2′-naphthol (BINOL)-based probes are very enantioselective for free amino acids due to their easily accessible chiral backbones and chemistry (Pu, 2004, 2017, 2020; Jo et al., 2014; Zhang et al., 2014). However, they typically respond to multiple analytes instead of one, meaning there is a lack of chemoselectivity. Meanwhile, most of those probes require the use of stoichiometric quantities of zinc(II) to form metal complexes and have associated disadvantages such as detection time and interference by metals (Huang et al., 2014; Zhu et al., 2019) (Scheme 1A and 1B). Previously, we reported a bisBINOL-based fluorescent sensor that can selectively respond to Arg, but it doesn't exhibit decent enantioselectivity (Yu et al., 2022). We believe that a new mechanism, much simplified experiments, and improved detection results can be achieved when a more active reaction site is incorporated (Scheme 1C). Acrylates, which are good electrophiles in Michael addition reactions and are applied broadly in polymer science (De et al., 2009; Farley et al., 2015), represent good candidates.

In this work, we have incorporated an acrylate into a fluorescent probe and discovered that it responds only to Arg both enantioselectively and chemoselectively, without the use of a metal ion to form complexes and within the timescale of minutes.

A Symmetric One Reaction Site (Huang et al., 2014)

(S)-**1**
Fluorescence OFF

Amino Acids / Zn(II), base → **Enantioselectivity**

Non-specific
Fluorescen ON

B Two Reaction Site (Zhu et al., 2019)

(S,S)-**2**
Fluorescence OFF

Amino Acids / Zn(II), base → **Enantioselectivity**

Non-specific
Fluorescen ON

C Three Reaction Site (This work)

(S)-**3**
Fluorescence OFF

Arg / Metal free Base free → **Enantioselectivity** **Chemoselectivity**

Specific
Fluorescence ON
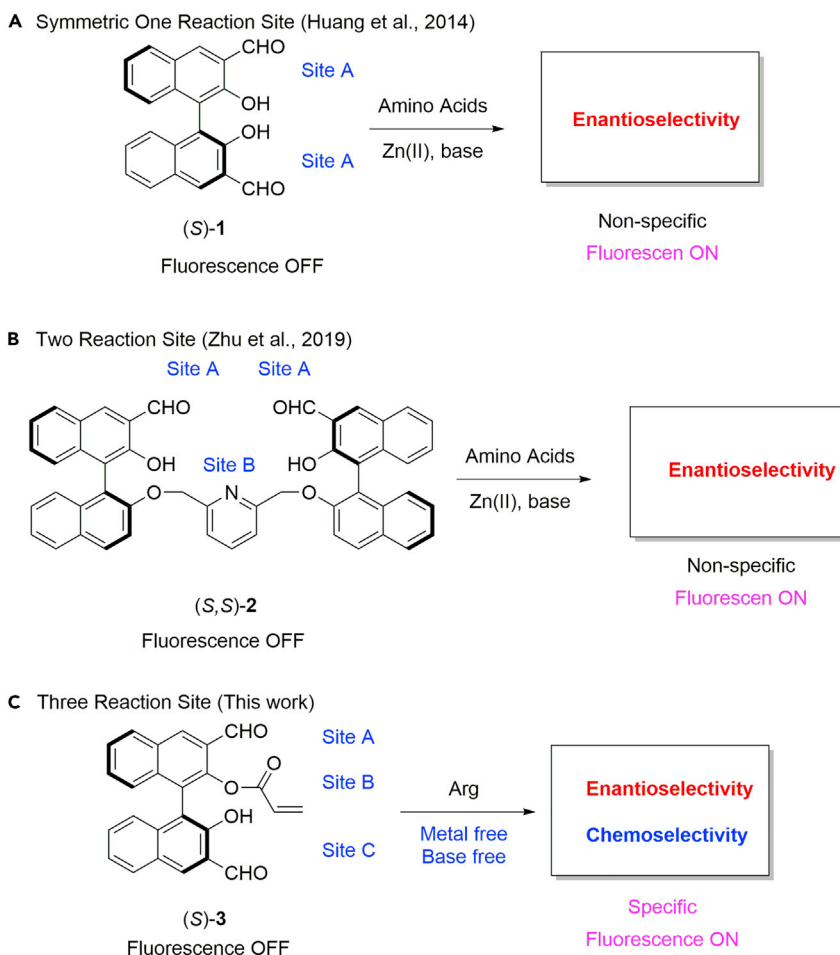
Scheme 1. General design of Arg-specific fluorescent probe

RESULTS AND DISCUSSION

Scheme 2 presents an efficient synthesis of the BINOL-based probe (S)-**3**. Treatment of (S)-BINOL with excess MOMBr (MOM = CH_3OCH_2) in the presence of sodium hydride gave the diMOM-protected BINOL (S)-**4**. Subsequent deprotonation with excess ^{n}BuLi and formylation with DMF gave the intermediate diformyl-diMOM-BINOL (S)-**5** after acidic workup. The MOM protecting group was then removed under acidic condition to give diformyl BINOL (S)-**1**. Reaction of (S)-**1** with acryloyl chloride in the presence of the weak organic base diisopropylethylamine gave (S)-**3** in 39% yield with a single acrylate on one side of the BINOL ring. Formation of (S)-**3** was evidenced by two singlet aldehyde protons at δ = 10.18 and 10.20 ppm, one singlet for the hydroxyl naphthenol proton at δ = 10.52 ppm, and three vinylic protons of the acrylate group at δ = 6.09 (dd, 1H, J = 17.3, 1.2 Hz), 5.92 (dd, 1H, J = 17.3, 10.4 Hz), and 5.66 (dd, 1H, J = 10.4, 1.3 Hz) ppm. No obvious fluorescence of (S)-**3** was observed in solution in DMSO.

The fluorescence response of (S)-**3** toward both enantiomers of free amino acids was investigated using DMSO as the solvent. A solution of (S)-**3** (50 μL, 1.6 mM in DMSO) was allowed to interact with 6 equiv of free amino acids (50 μL, 9.6 mM in water) in the presence of 300 μL DMSO to form homogeneous solution. The reaction mixture was allowed to stand at room temperature for 300 s (see Figures S1–S5), after which it was diluted with DMSO (3.6 mL) and fluorescence measured. The final concentration of the probes in the solutions was 2.0×10^{-5} M.

Figure 1 summarizes the fluorescence data where the peak intensity at λ = 525 nm was compared. When (S)-**3** was treated with most amino acids as both of their enantiomers, only a very small fluorescence
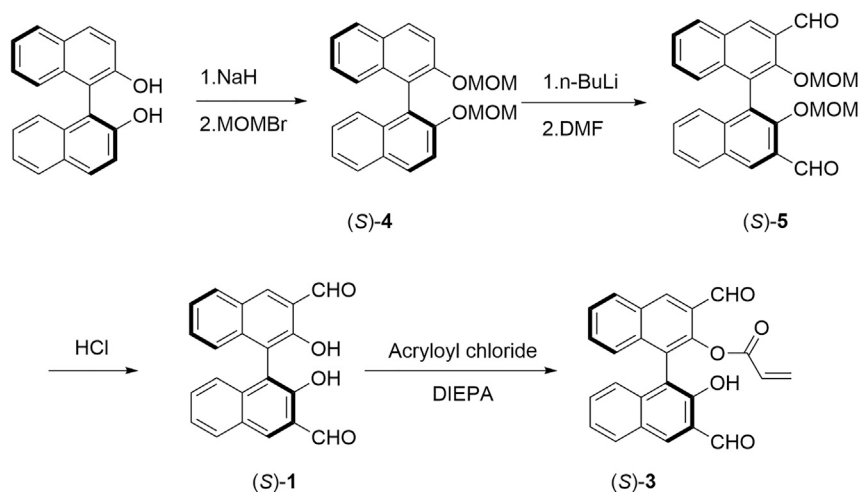
Scheme 2. Synthesis of the fluorescent probe (S)-3

enhancement was observed (See Figures S18–S36). However, fluorescence at λ = 525 nm was enhanced greatly with D-Arg and its intensity was found to be 528% greater than that with L-Arginine (L-Arg). The enantioselective factor [$ef = (I_D-I_0)/(I_L-I_0)$, where I_L, I_D, and I_0 are the fluorescence intensity toward L-amino acids, D-amino acids, and the probe itself, respectively] was calculated to be 487. Chemoselectivity was also observed so that the fluorescence response of (S)-3 toward D-Arg was much higher than for any other amino acids as either enantiomer as shown in Figure 1A. Thus, probe (S)-3 responded only to D-Arg.

We then studied how (S)-3 would respond to L- and D-Arg by titrating with stock solutions of known concentration (see Figures S6–S9). As shown in Figure 2A, the fluorescence intensity increased with increasing Arg concentration up to 5 equiv L- or D-Arg at which the fluorescence enhancement was saturated. In the range of 0 to 5 equiv of either enantiomer, a linear, first-order fit was applied and a value of $R^2 > 0.99$ was found. The limit of detection (LOD) was thus determined to be 50 nM for D-Arg (LOD = 3*SD/k, where SD is the standard deviation of the noise and k is the slope of the calibration curve). Analogous experiments were then conducted under the same conditions using (R)-3, and the data, which are shown as Figures 2B and 2D, show the inverse response with strong fluorescence enhancement in the presence of L-Arg. This confirms that the observed differential fluorescent response of the sensor toward Arg enantiomers is due to chiral discrimination.
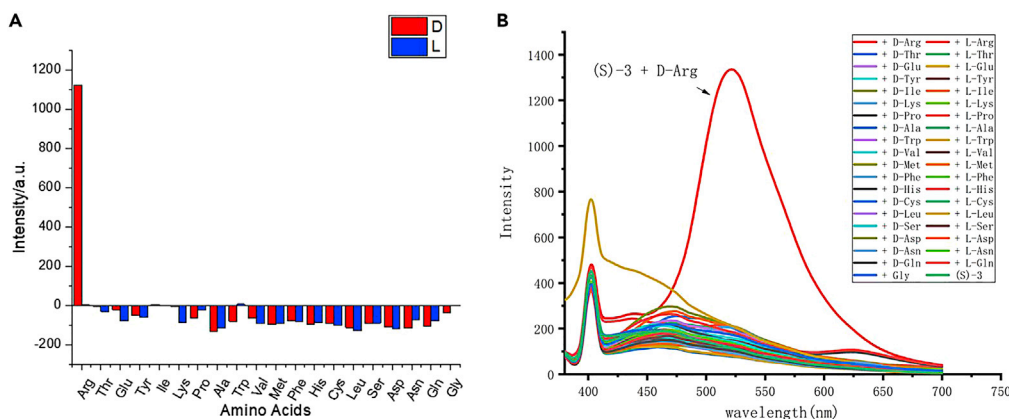

Figure 1. The fluorescence data where the peak intensity at λ = 525 nm was compared
(A) Fluorescence intensity of (S)-3 (0.02 mM) with addition of L- or D-amino acids in DMSO.
(B) Fluorescence response of (S)-3 (0.02 mM) with addition of 6 equiv L- or D- amino acids in DMSO (containing 1.25% DCM and 1.25% water). (λ_{em} = 525 nm, λ_{ex} = 360 nm, slit = 3.0/3.0 nm, t = 300 s).
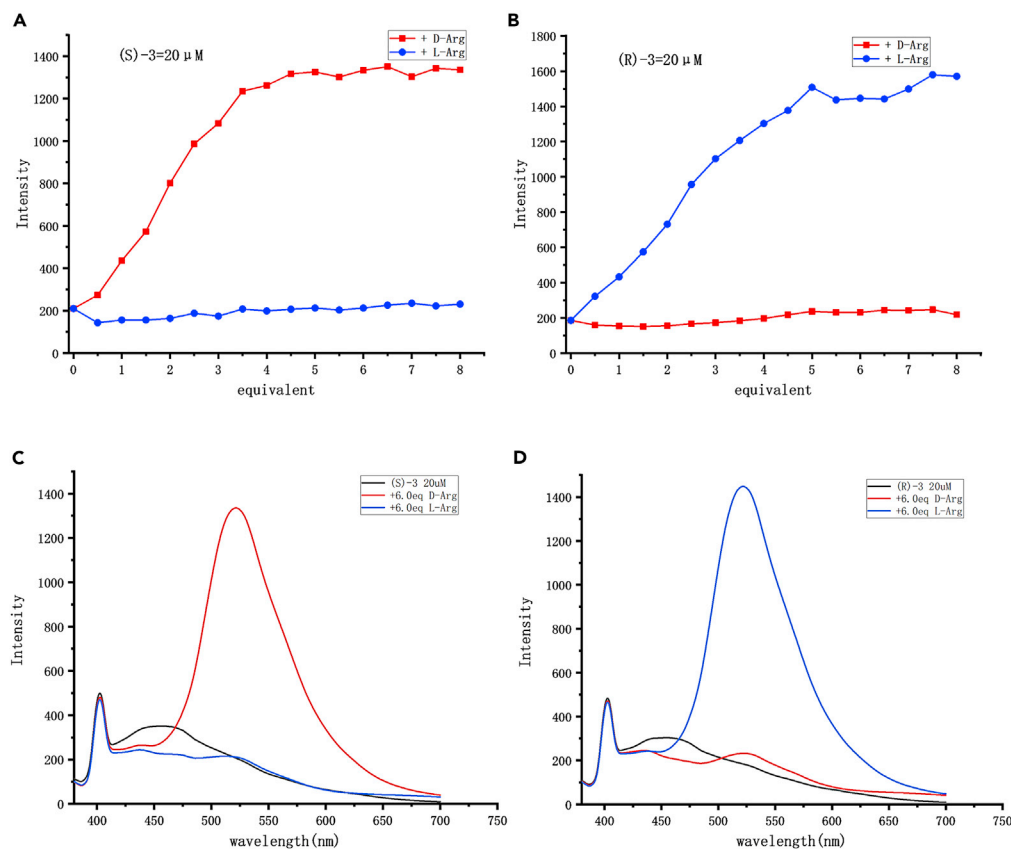
Figure 2. Chiral of sensor led to different fluorescent response of Arg enantiomers
(A) The fluorescence responses of (S)-**3** toward various concentration of L- and D-Arg.
(B) The fluorescence responses of (R)-**3** toward various concentration of L- and D-Arg.
(C) The fluorescence spectrum of (S)-**3** in the presence of 6.0 equiv of L- or D-Arg.
(D) The fluorescence spectrum of (R)-**3** in the presence of 6.0 equiv of L- or D-Arg. Solvent = DMSO (containing 1.25% DCM and 1.25% water). (λ_{em} = 525 nm, λ_{ex} = 360 nm, slit = 3.0/3.0 nm, t = 300 s).

With an Arg detection range of 5 to 400 μM, (S)-**3** is then potentially useful for the measurement of Arg concentrations in biological systems such as human serum, where Arg is found to be around 70–100 μM (Möller et al., 1979, 1983).

Next we studied the fluorescence response of Arg solutions at various different enantiomeric excesses (ee = [D-L]/[D + L]). As shown in Figure 3, the fluorescence responses of (S)-**3** and (R)-**3** exhibit a nearly mirror-image relationship. In common with the studies illustrated in Figure 2, this ee study further confirms the observed enantioselective recognition.

Surprisingly, we also found that Arg can be differentiated by the naked eye. Thus, upon addition of D-Arg, the probe solution adopted a dark brown color, (see Figure 4A) while L-Arg caused the solution to turn light brown. None of the other amino acids change the color significantly. This phenomenon indicated a quite different mechanism of the reaction between probe (S)-**3** with Arg. And we believe it's the strong UV-vis absorption of 400–500 nm that leads to the orange-red color upon interaction with Arg.

UV-vis, NMR, and MS studies were carried out to provide insights into the mechanism (see Figures S10–S17). Upon increasing concentration of D- and L-Arg, similar increase at 300 nm and 380 nm was observed. The UV-vis data indicated similarity in the products' conjugation with either D- or L-Arg (See Figure S10). Kinetic NMR studies confirmed the fast reaction between the probes with Arg (see Figures S16 and S17). Both enantiomers of Arg finished reactions with the probe within 60 s. The reaction between (S)-**3** and
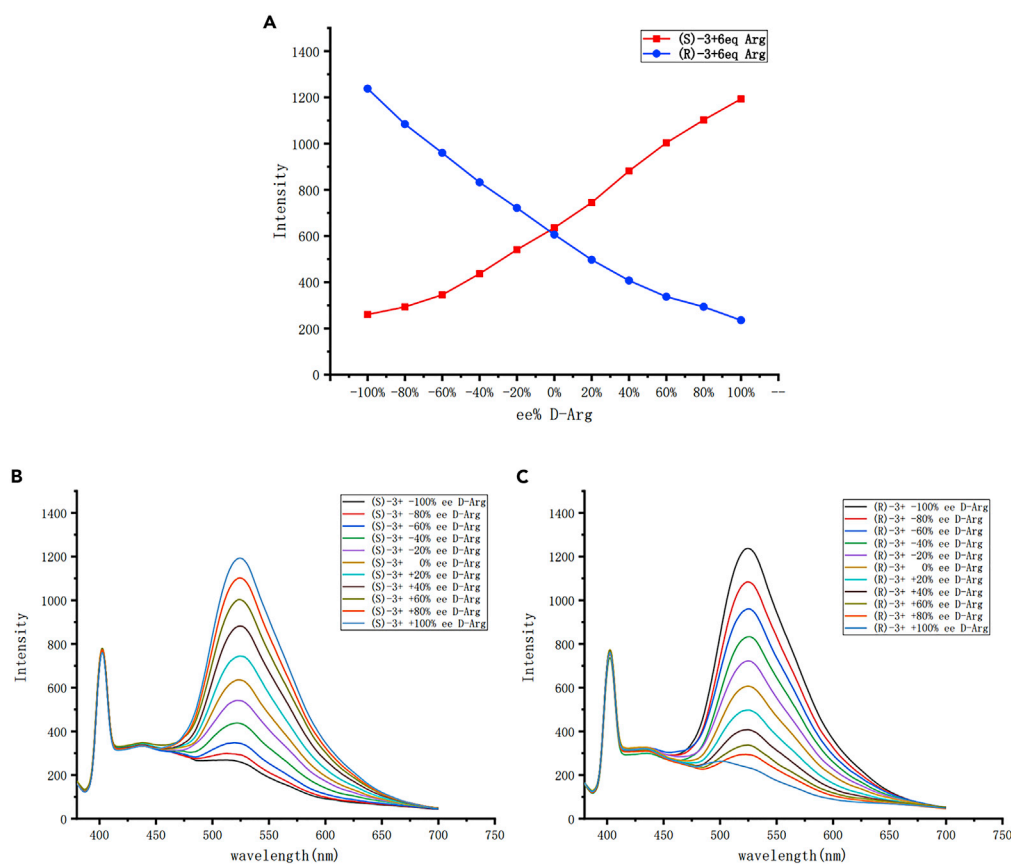
Figure 3. Enantioselective fluorescence enhancement of arginine enantiomers by chiral sensors

(A) Fluorescence intensity at 525 nm was plotted against various ee of Arg.

(B) The fluorescence responses of (S)-**3** (0.02 mM) toward various ee of Arg.

(C) The fluorescence responses of (R)-**3** (0.02 mM) toward various ee of Arg in DMSO (containing 1.25% DCM and 1.25% water). (λ_{em} = 525 nm, λ_{ex} = 360 nm, slit = 3.0/3.0 nm, t = 300 s).

L-Arg yields two sets of acrylate signal with a ratio of 80:20 (acrylate ion vs. aromatic acrylate), while (S)-**3** and D-Arg yields mostly only one set of acrylate protons (acrylate ion). Another key observation is that the aromatic protons' signals became more symmetric, indicating the majority of the products with both D-/L-Arg are symmetric imine product with the acrylate ester bond cleaved. Considering the fact that the imine products are mostly nonemissive and that both acrylate ion and Arg are not emissive, we hypothesized the formation of possible 1,4-Michael addition product of the acrylate between (S)-**3** and D-Arg but not with (S)-**3** and L-Arg. As long as MS data (See Figures S11 and S12), we proposed some possible products between the reaction of the probe and Arg in scheme 3.

Computational studies have shown the relative energy of those possible reaction products (See Figures S37–S42). In the reaction between (S)-**3** and D-Arg, the possible cyclic product (S)-**3**/D-Arg-3 was favored by 0.036 eV than (S)-**3**/D-Arg-1 and by 0.22 eV than (S)-**3**/D-Arg-2. While in the reaction between (S)-**3** and L-Arg, the possible product (S)-**3**/L-Arg-2 was favored by 0.07–0.08 eV than other two possible products (see Table 1). The data supported the formation of a cyclic product between (S)-**3** and D-Arg only. Particularly, the HOMO of (S)-**3**/D-Arg-3 locates predominantly on Arg's guanidino group and the LUMO locates mostly on one naphthalene ring of the BINOL. However, the HOMO and LUMO of (S)-**3**/L-Arg locate nearly only on BINOL. This distinct difference of HOMO/LUMO distribution could help understand why (S)-**3** can enantioselectively recognize D-Arg (see Figure 5). Intramolecular charge transfer (ICT) is highly possible to happen among (S)-**3**/D-Arg, and it is rationalized to be responsible for the fluorescence enhancement observations. While other amino
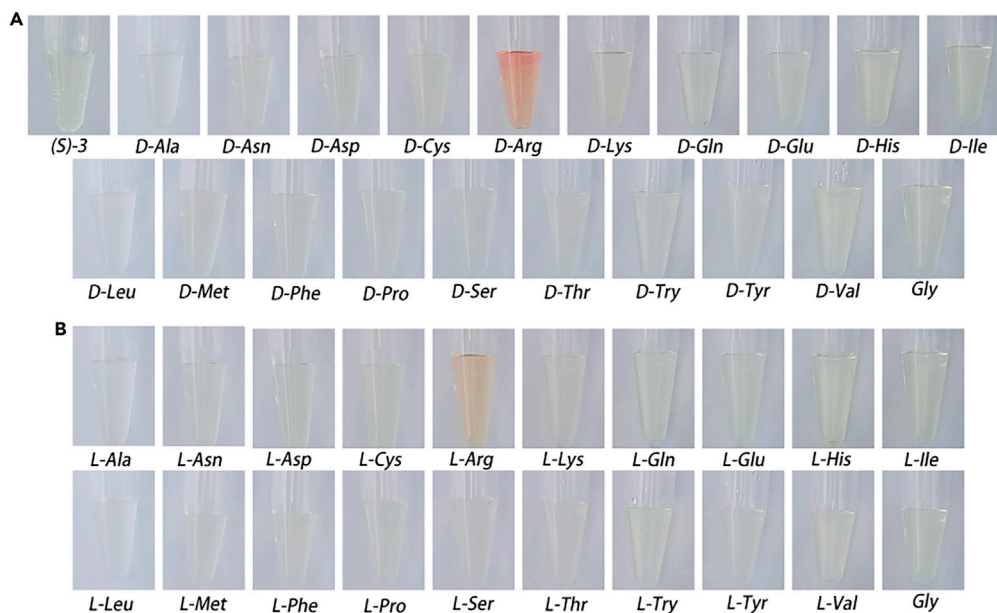
Figure 4. The colorimetric detection experiment of (S)-3

Colorimetric detection of (A) D-amino acids (6 eq.);(B) L-amino acids (6 eq.). In DMSO with (S)-3 (0.02 mM) (with 1.25% DCM and 1.25% water, t = 300 s).

acids do not have comparable functional groups as Arg, it is hypothesized that the ICT also contributes to the chemoselectivity for Arg.

Conclusion

In conclusion, a BINOL-based fluorescent probe bearing multiple active detection sites was synthesized efficiently. It can specifically detect chiral Arg among 39 structurally similar amino acids, both chemoselectively among 20 types of amino acids and enantioselectively among their enantiomers with an ef value of 487. To our knowledge, this is the first time such a specific fluorescent probe for chiral Arg that has been reported. The unprecedented specificity was rationalized to come from the acrylate of the probe, an additional reaction site that only forms a cyclic compound with a certain enantiomer of Arg. Computational studies supported the hypothesis that the formed Michael addition product, although not in abundance, experienced a strong ICT to emit strong fluoresce and contributed to the selectivity. Comparing with other enantioselective fluorescent probes that were used to detect chiral amino acids, this probe has advantages such as the specificity for
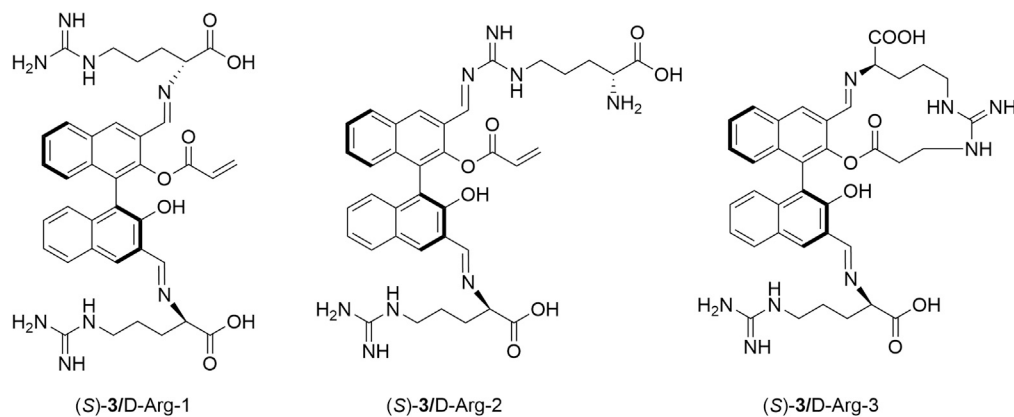
Scheme 3. Possible products of the sensing reactions

Table 1. Calculated relative energy of the sensing products

	(S)-3/ L-ARG-1	(S)-3/ L-ARG-2	(S)-3/ L-ARG-3	(S)-3/ D-ARG-1	(S)-3/ D-ARG-2	(S)-3/ D-ARG-3
HOMO/EV	0.068	0.000	0.081	0.036	0.220	0.000
LUMO/EV	0.032	0.000	0.043	0.161	0.097	0.000

Arg, metal-free detection, quick responses, and the ability for colorimetric detection. We believe the specificity of this probe could encourage biological and industrial applications of enantioselective probes.

Limitations of the study

However, the fluorescent probe (S)-3 exhibited decent enantioselectivity and chemoselectivity for Arg. Limitations should be noted such that the experimental media were limited mostly in organic solvents. The weak fluorescence in aqueous studies probably came from the fact that final imine products were not stable there.

STAR★METHODS

Detailed methods are provided in the online version of this paper and include the following:

- KEY RESOURCES TABLE
- RESOURCE AVAILABILITY
  - Lead contact
  - Materials availability
  - Data and code availability
- EXPERIMENTAL MODEL AND SUBJECT DETAILS
- METHOD DETAILS
  - Materials and instrumentation
  - Synthesis and characterization of compounds
  - Preparation of samples for fluorescence measurements
  - Preparation of samples for UV-Vis absorption measurements
  - Preparation of samples for mass spectra measurements
  - Preparation of samples for NMR spectra measurements
  - The method of molecular modeling studies on the (S)-3/D- and L-Arg

SUPPLEMENTAL INFORMATION

Supplemental information can be found online at https://doi.org/10.1016/j.isci.2022.104964.
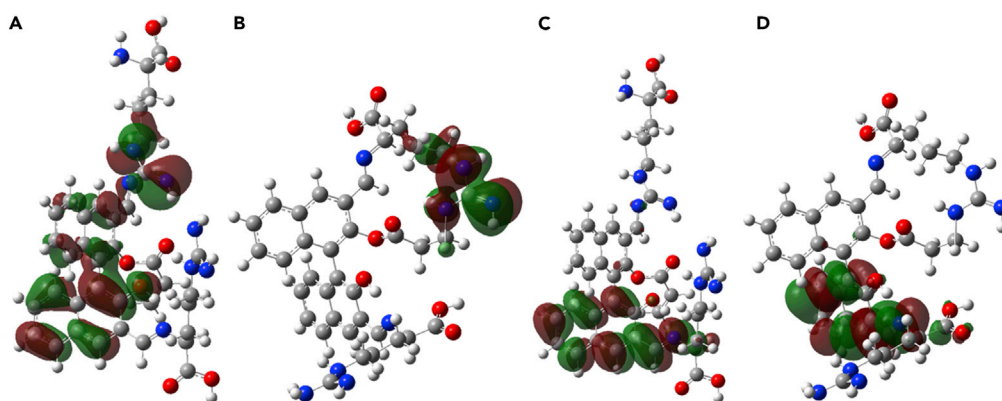
Figure 5. The HOMO and LUMO of (S)-3/ Arg
(A) HOMO of (S)-3/L-Arg-2.
(B) HOMO of (S)-3/D-Arg-3.
(C) LUMO of (S)-3/L-Arg-2.
(D) LUMO of (S)-3/D-Arg-3.

AUTHOR CONTRIBUTIONS

Conceptualization, X.Y., G.D., and C.Z.; Methodology, X.Y, B.Z., Q.Y., and S.W.; Software, H.H. and Q.D.; Validation, G.D. and C.Z.; Formal analysis, X.Y., B.Z., C.F., G.D., and C.Z.; Investigation, X.Y. and B.Z.; Resources, Y.G. and C.Z.; Writing – original draft preparation, X.Y. and G.D.; Writing – review and editing, G.D., Y.G., and C.Z.; Supervision, G.D. and C.Z. All authors have read and agreed to the published version of the manuscript.

DECLARATION OF INTERESTS

The authors declare no competing interests.

REFERENCES

Alvarez, L., Aliashkevich, A., De Pedro, M.A., and Cava, F. (2018). Bacterial secretion of D-arginine controls environmental microbial biodiversity. ISME J. *12*, 438–450.

Balu, D.T., Li, Y., Puhl, M.D., Benneyworth, M.A., Basu, A.C., Takagi, S., Bolshakov, V.Y., and Coyle, J.T. (2013). Multiple risk pathways for schizophrenia converge in serine racemase knockout mice, a mouse model of NMDA receptor hypofunction. Proc. Natl. Acad. Sci. USA *110*, 2400–2409.

Balu, D.T., Takagi, S., Puhl, M.D., Benneyworth, M.A., and Coyle, J.T. (2014). D-serine and serine racemase are localized to neurons in the adult mouse and human forebrain. Cell. Mol. Neurobiol. *34*, 419–435.

Beltrán-Castillo, S., Olivares, M.J., Contreras, R.A., Zúñiga, G., Llona, I., Von Bernhardi, R., and Eugenín, J.L. (2017). D-serine released by astrocytes in brainstem regulates breathing response to CO_2 levels. Nat. Commun. *8*, 838.

Chen, C.L., Hsu, S.C., Chung, T.Y., Chu, C.Y., Wang, H.J., Hsiao, P.W., Yeh, S.D., Ann, D.K., Yen, Y., and Kung, H.J. (2021). Arginine is an epigenetic regulator targeting TEAD4 to modulate OXPHOS in prostate cancer cells. Nat. Commun. *12*, 2398.

Chen, J., Ou, Y., Yang, Y., Li, W., Xu, Y., Xie, Y., and Liu, Y. (2018). KLHL22 activates amino-acid-dependent mTORC1 signalling to promote tumorigenesis and ageing. Nature *557*, 585–589.

Dai, X., Zhou, E., Yang, W., Zhang, X., Zhang, W., and Rao, Y. (2019). D-Serine made by serine racemase in drosophila intestine plays a physiological role in sleep. Nat. Commun. *10*, 1986.

D'Aniello, A. (2007). D-Aspartic acid: an endogenous amino acid with an important neuroendocrine role. Brain Res. Rev. *53*, 215–234.

De, K., Legros, J., Crousse, B., and Bonnet-Delpon, D. (2009). Solvent-promoted and -controlled aza-michael reaction with aromatic amines. J. Org. Chem. *74*, 6260–6265.

Farley, A.J.M., Sandford, C., and Dixon, D.J. (2015). Bifunctional iminophosphorane catalyzed enantioselective sulfa-michael addition to unactivated α-substituted acrylate esters. J. Am. Chem. Soc. *137*, 15992–15995.

Garton, M., Nim, S., Stone, T.A., Wang, K.E., Deber, C.M., and Kim, P.M. (2018). Method to generate highly stable D-amino acid analogs of bioactive helical peptides using a mirror image of the entire PDB. Proc. Natl. Acad. Sci. USA *115*, 1505–1510.

Henneberger, C., Papouin, T., Oliet, S.H.R., and Rusakov, D.A. (2010). Long-term potentiation depends on release of D-serine from astrocytess. Nature *463*, 232–236.

Huang, Z., Yu, S., Wen, K., Yu, X., and Pu, L. (2014). Zn(II) promoted dramatic enhancement in the enantioselective fluorescent recognition of functional chiral amines by a chiral aldehyde. Chem. Sci. *5*, 3457–3462.

Jo, H.H., Lin, C.Y., and Anslyn, E.V. (2014). Rapid optical methods for enantiomeric excess analysis: from enantioselective indicator displacement assays to exciton-coupled circular dichroism. Acc. Chem. Res. *47*, 2212–2221.

Lemos, H., Huang, L., Prendergast, G.C., and Mellor, A.L. (2019). Immune control by amino acid catabolism during tumorigenesis and therapy. Nat. Rev. Cancer *19*, 162–175.

Maze, I., Noh, K.M., Soshnev, A.A., and Allis, C.D. (2014). Every amino acid matters: essential contributions of histone variants to mammalian development and disease. Nat. Rev. Genet. *15*, 259–271.

Möller, P., Alvestrand, A., Bergström, J., Fürst, P., and Hellström, K. (1983). Electrolytes and free amino acids in leg skeletal muscle of young and elderly women. Gerontology *29*, 1–8.

Möller, P., Bergström, J., Eriksson, S., Fürst, P., and Hellström, K. (1979). Effect of aging on free amino acids and electrolytes in leg skeletal muscle. Clin. Sci. *56*, 427–432.

Murray, P.J. (2016). Amino acid auxotrophy as a system of immunological control nodes. Nat. Immunol. *17*, 132–139.

Neame, S., Safory, H., Radzishevsky, I., Touitou, A., Marchesani, F., Marchetti, M., Kellner, S., Berlin, S., Foltyn, V.N., Engelender, S., et al. (2019). The NMDA receptor activation by d-serine and glycine is controlled by an astrocytic Phgdh-dependent serine shuttle. Proc. Natl. Acad. Sci. USA *116*, 20736–20742.

Pu, L. (2004). Fluorescence of organic molecules in chiral recognition. Chem. Rev. *104*, 1687–1716.

Pu, L. (2017). Simultaneous determination of concentration and enantiomeric composition in fluorescent sensing. Acc. Chem. Res. *50*, 1032–1040.

Pu, L. (2020). Enantioselective fluorescent recognition of free amino acids: challenges and opportunities. Angew. Chem. Int. Ed. Engl. *59*, 21814–21828.

Sasabe, J., Miyoshi, Y., Rakoff-Nahoum, S., Zhang, T., Mita, M., Davis, B.M., Hamase, K., and Waldor, M.K. (2016). Interplay between microbial

D-amino acids and host D-amino acid oxidase modifies murine mucosal defence and gut microbiota. Nat. Microbiol. *1*, 16125.

Shmueli, M.D., Levy-Kanfo, L., Haj, E., Schoenfeld, A.R., Gazit, E., and Segal, D. (2019). Arginine refolds, stabilizes, and restores function of mutant pVHL proteins in animal model of the VHL cancer syndrome. Oncogene *38*, 1038–1049.

Sievers, S.A., Karanicolas, J., Chang, H.W., Zhao, A., Jiang, L., Zirafi, O., Stevens, J.T., Münch, J., Baker, D., and Eisenberg, D. (2011). Structure-based design of non-natural amino-acid inhibitors of amyloid fibril formation. Nature *475*, 96–100.

Yu, X., Zhang, B., Liao, P., Huang, J., Fan, C., Hu, H., Dong, Q., Du, G., Gao, Y., and Zeng, C. (2022). A chemoselective fluorescent probe for arginine in aqueous phase. Dyes Pigments *203*, 110339.

Zhang, X., Yin, J., and Yoon, J. (2014). Recent advances in development of chiral fluorescent and colorimetric sensors. Chem. Rev. *114*, 4918–4959.

Zhu, Y.Y., Wu, X.D., Gu, S.X., and Pu, L. (2019). Free amino acid recognition: a bisbinaphthyl-based fluorescent probe with high enantioselectivity. J. Am. Chem. Soc. *141*, 175–181.

STAR★METHODS

KEY RESOURCES TABLE

REAGENT or RESOURCE	SOURCE	IDENTIFIER
Chemicals, peptides, and recombinant proteins		
(S)-BINOL	Aladdin	CAS: 18531-99-2
(R)-BINOL	Aladdin	CAS: 18531-94-7
L-Ala	Innochem	CAS: 56-41-7
L-Arg	Innochem	CAS: 74-79-3
L-Asn	Innochem	CAS: 70-47-3
L-Asp	Innochem	CAS: 56-84-8
L-Cys	Innochem	CAS: 52-90-4
L-Gln	Innochem	CAS: 56-85-9
L-Glu	Innochem	CAS: 56-86-0
Gly	Innochem	CAS: 56-40-6
L-His	Innochem	CAS: 71-00-1
L-Ile	Innochem	CAS: 73-32-5
L-Leu	Innochem	CAS: 61-90-5
L-Lys	Innochem	CAS: 56-87-1
L-Met	Innochem	CAS: 63-68-3
L-Phe	Innochem	CAS: 63-91-2
L-Pro	Innochem	CAS: 147-85-3
L-Ser	Innochem	CAS: 56-45-1
L-Thr	Innochem	CAS: 72-19-5
L-Try	Innochem	CAS: 73-22-3
L-Tyr	Innochem	CAS: 60-18-4
L-Val	Innochem	CAS: 72-18-4
D-Ala	Innochem	CAS: 338-69-2
D-Arg	Innochem	CAS: 157-06-2
D-Asn	Innochem	CAS: 2058-58-4
D-Asp	Innochem	CAS: 1783-96-6
D-Cys	Innochem	CAS: 921-01-7
D-Gln	Innochem	CAS: 5959-95-5
D-Glu	Innochem	CAS: 6893-26-1
D-His	Innochem	CAS: 351-50-8
D-Ile	Innochem	CAS: 319-78-8
D-Leu	Innochem	CAS: 328-38-1
D-Lys	Innochem	CAS: 923-27-3
D-Met	Innochem	CAS: 348-67-4
D-Phe	Innochem	CAS: 673-06-3
D-Thr	Innochem	CAS: 632-20-2
D-Try	Innochem	CAS: 153-94-6
D-Tyr	Innochem	CAS: 556-02-5
D-Val	Innochem	CAS: 640-68-6
Sodium sulfate	Macklin	CAS: 7757-82-6

Continued

REAGENT or RESOURCE	SOURCE	IDENTIFIER
Sodium chloride	Macklin	CAS: 7647-14-5
Sodium hydride	Meryer	CAS: 7646-69-7
Silica gel	Qingdao Gulf Fine Chemical Co., Ltd.	CAS: 112926-00-8
Acryloyl chloride	Innochem	CAS: 814-68-6
Diisopropylethylamine	Innochem	CAS: 7087-68-5
Bromomethyl methyl ether	ADAMAS	CAS: 13057-17-5
n-BuLi	damas-beta	CAS: 109-72-8
HCl	Xilong Chemical Co., Ltd.	CAS: 7647-01-0
Dichloromethane	GENERAL-REAGENT	CAS: 75-09-2
Petroleum ether	GENERAL-REAGENT	CAS: 8032-32-4
Ethyl acetate	GENERAL-REAGENT	CAS: 141-78-6
N,N-Dimethylformamide	Innochem	CAS: 68-12-2
Tetrahydrofuran	Aladdin	CAS: 109-99-9
Methanol	GENERAL-REAGENT	CAS: 67-56-1
Ethanol	GENERAL-REAGENT	CAS: 64-17-5
Acetonitrile	Innochem	CAS: 75-05-8
Dimethyl sulfoxide	Innochem	CAS: 67-68-5
Software and algorithms		
Origin 2018	OriginLab	https://www.originlab.com/
ChenBioDraw 14	PerkinElmer	https://perkinelmerinformatics.com/products/research/chemdraw/
MestReNova	Mestrelab	https://mestrelab.com/
Spectra Manager II	JASCO	http://www.jasco.co.jp/

RESOURCE AVAILABILITY

Lead contact

All requests for reagents and resources should be directed to the lead contact, Chaoyuan Zeng (zengchaoyuan@hainanu.edu.cn).

Materials availability

Synthetic routes to all chemical compounds are described in supplemental information. Where available, these may be shared by the lead contact. Solvent, reagents, and amino acids used for the fluorescence detection studies were obtained from the commercial or internal sources described in the key resources table.

Data and code availability

- All data reported in this paper will be shared by the lead contact upon request.

- This paper does not report original code.

- Any additional information required to reanalyze the data reported in this paper is available from the lead contact upon request.

EXPERIMENTAL MODEL AND SUBJECT DETAILS

(*S*)-**3** achieves specific fluorescence recognition of D-Arg in 39 amino acids.

METHOD DETAILS

Materials and instrumentation

All reactions were carried out under N_2 unless otherwise noted. Chemicals were purchased from Meryer (Shanghai) Chemical Technology Co. or Beijing Innochem Science & Technology co. THF were distilled with sodium wire to dry it. NMR spectra were recorded on AVANCE NEO 400 MHz spectrometer. Steady-state fluorescence emission spectra were recorded on JASCO spectrofluorometer FP-8650 .

Synthesis and characterization of compounds

Synthesis of (S)-2,2'-bis(methoxymethoxy)-1,1'-binaphthalene (S)-4

NaH (50 mmol, 2 g) was dispersed in dry THF (30 mL). The solution was cooled to 0°C, and (S)-BINOL (18 mmol, 5 g) in dry THF (10 mL) was added to the mixture dropwise. The mixture was warmed up to room temperature to react for additional 2 h. Then the solution was cooled to 0°C again, at which MOMOBr (75.8 mmol, 6.2 mL) was added to the solution dropwise, then it was warmed up to room temperature to react overnight. 20 mL H_2O was added to quench the reaction at 0°C. The organic layer was separated, and the aqueous layer was extracted with ethyl acetate (3 × 20 mL). The combined organic layers were dried over anhydrous Na_2SO_4. After evaporation of the solvents, recrystallize the crude product from methanol to yield 4.9 g (73%) (S)-4 as white solid (Huang et al., 2014).

Synthesis of (S)-2,2'-bis(methoxymethoxy)-[1,1'-binaphthalene]-3,3'-dicarbaldehyde (S)-5

(S)-4 (5.34 mmol, 2 g) was dissolved in dry THF (30 mL). The solution was cooled to −78°C, and n-BuLi (13.35 mmol, 8.3 mL, 1.6 M in hexane) was added dropwise. The reaction mixture was stirred at room temperature for 2 h. Then it was cooled to 0°C, DMF (12.82 mmol, 1 mL) was added dropwise. The reaction mixture was warmed up to room temperature to react for additional 1 h. Saturated NH_4Cl (2 mL) was added to quench the reaction at 0°C. The organic layer was separated, and the aqueous layer was extracted with ethyl acetate (3 × 20 mL). The combined organic extracts were washed with brine, and dried over anhydrous Na_2SO_4. After evaporation of the solvents, the residue was purified by column chromatography on silica gel eluted with petroleum ether/ethyl acetate (10/1) to afford crude compound (S)-5 as a yellow oil, and the crude was used for next step (Huang et al., 2014).

Synthesis of (S)-2,2'-dihydroxy-[1,1'-binaphthalene]-3,3'-dicarbaldehyde (S)-1

Concentrated HCl (15 mL) was added dropwise to a solution of (S)-5 in DCM/ethanol (60mL, 1:1). After stirring overnight, $NaHCO_3$ solid was added to quench the reaction until no bubbles appear. The organic layer was separated, and the aqueous layer was extracted with DCM (3 × 20 mL). The combined organic extracts were washed with brine, and dried over anhydrous Na_2SO_4. After evaporation of the solvents, 800 mg yellow solid (S)-1 was obtained in 40% yield for two steps. ^{1}H NMR (400 MHz, $CDCl_3$) δ 10.58 (s, 2H), 10.20 (s, 2H), 8.35 (s, 2H), 8.00 (dd, J = 6.4, 3.0 Hz, 2H), 7.45–7.39 (m, 4H), 7.20 (dd, J = 6.9, 2.8 Hz, 2H) (Huang et al., 2014).

Synthesis of (S)-3,3'-diformyl-2'-hydroxy-[1,1'-binaphthalen]-2-yl acrylate (S)-3

(S)-1 (0.35 mmol, 120 mg) was dissolved in dry acetonitrile (30 mL). The solution was cooled to 0°C, and DIEPA (0.88 mmol, 144.8 uL) was added dropwise. The reaction mixture was stirred at room temperature for 3 h. Then it was cooled to 0°C, at which acryloyl chloride (0.42 mmol, 34.2 uL) was added dropwise. The reaction mixture was warmed up to room temperature overnight. Saturate NH_4Cl (30 mL) was added to quench the reaction, then the organic layer was separated, and the aqueous layer was extracted with DCM (3 × 10 mL). The combined organic extracts were dried over anhydrous Na_2SO_4. After evaporation of the solvents, the residue was purified by column chromatography on silica gel eluted with DCM to afford compound (S)-3 as a yellow solid in 39% yield.

^{1}H NMR (400 MHz, $CDCl_3$) δ 10.45 (s, 1H), 10.12 (s, 1H), 10.10 (s, 1H), 8.52 (s, 1H), 8.25 (s, 1H), 8.05 (d, J = 8.2 Hz, 1H), 7.91–7.86 (m, 1H), 7.50 (t, J = 7.0 Hz, 1H), 7.39 (t, J = 7.0 Hz, 1H), 7.35–7.30 (m, 2H), 7.22 (d, J = 8.4 Hz, 1H), 7.11 (dd, J = 6.0, 2.9 Hz, 1H), 6.04 (d, J = 16.1 Hz, 1H), 5.84 (dd, J = 17.3, 10.4 Hz, 1H), 5.60 (d, J = 11.7 Hz, 1H). ^{13}C NMR (101 MHz, $CDCl_3$) δ 195.53, 187.91, 162.98, 152.57, 144.56, 137.67, 136.12, 134.98, 134.21, 131.57, 130.12, 129.77, 129.16, 128.87, 128.69, 126.54, 126.26, 125.90, 125.82, 124.92, 124.85, 124.15, 123.63, 120.71, 114.60.HRMS (TOF ES+): calcd for $C_{25}H_{16}O_5$ (MH+), 397.1071; found, 397.1067. Mp: 178–180°C $[\alpha]_D^{25}$ = −53.9 (c = 0.56 mg/mL, CH_2Cl_2).

Synthesis of (R)-3,3'-diformyl-2'-hydroxy-[1,1'-binaphthalen]-2-yl acrylate (R)-3

(R)-**3** was synthesized following the same method mentioned above except that (R)-BINOL was used instead of (S)-BINOL. ^{1}H NMR (400 MHz, CDCl$_3$) δ 10.52 (s, 1H), 10.20 (s, 1H), 10.18 (s, 1H), 8.60 (s, 1H), 8.33 (s, 1H), 8.13 (d, J = 8.2 Hz, 1H), 7.96 (d, J = 9.3 Hz, 1H), 7.58 (t, J = 7.5 Hz, 1H), 7.49 – 7.44 (m, 1H), 7.42–7.39 (m, 2H), 7.29 (d, J = 8.5 Hz, 1H), 7.18 (d, J = 9.4 Hz, 1H), 6.11 (d, J = 17.2 Hz, 1H), 5.91 (dd, J = 17.3, 10.4 Hz, 1H), 5.67 (d, J = 10.5 Hz, 1H). ^{13}C NMR (101 MHz, CDCl$_3$) δ195.54, 187.97, 163.01, 152.57, 144.54, 137.68, 136.12, 134.98, 134.27, 131.61, 130.12, 129.79, 129.17, 128.89, 128.70, 126.52, 126.25, 125.92, 125.81, 124.92, 124.84, 124.16, 123.64, 120.70, 114.59.HRMS (TOF ES+): calcd for C$_{25}$H$_{16}$O$_5$ (MH$^+$), 397.1071; found, 397.1075. Mp: 180–182°C $[\alpha]_D^{25}$= 54.9 (c = 0.56 mg/mL, CH$_2$Cl$_2$).

Preparation of samples for fluorescence measurements

Prepare fresh stock solutions of 1.6mM (S)-**3** and 9.6 mM amino acids in DCM and ultrapure water for each measurement. In the fluorescence enhancement study, the (S)-**3** stock solution was added to a 5 mL test tube, followed by the addition of the amino acid solution with designated equivalences. Extra DMSO was added to keep the total volume of the solution at 0.4 mL. The solution was allowed to react at room temperature for 300 s before being diluted to 4 mL with DMSO, unless otherwise noted.

Preparation of samples for UV-Vis absorption measurements

In the UV-Vis absorption study, the (S)-**3** stock solution was added to a 5 mL test tube, followed by the addition of the Arginine solution with designated equivalences. Extra DMSO was added to keep the total volume of the solution at 0.4 mL. The solution was allowed to react at room temperature for 300 s before being diluted to 4 mL with DMSO, unless otherwise noted.

Preparation of samples for mass spectra measurements

In the Mass spectra study, weigh (S)-**3** (3 mg) and dissolve in 0.5 mL DMSO, then weigh D-Arg (41.6 mg) and dissolve in 0.5 mL ultrapure water. Add 62.5 µL D-Arg to (S)-**3** of DSMO solution. After mixing uniformly, react for 7h. Dilute the sample before proceeding with mass spectrometry. L-Arg operation is the same as D-Arg.

Preparation of samples for NMR spectra measurements

In the NMR spectra study, weigh (S)-**3** (3 mg) and dissolve in 0.5mL DMSO, then weigh D-Arg (41.6 mg) and dissolve in 0.5 mL ultrapure water. Add 62.5 µL D-Arg to (S)-**3** of DSMO solution. After mixing uniformly, react for 60s, 300s, 10min, 30min, 1h, 3h, 5h and 7hfor NMR spectra study. L-Arg operation is the same as D-Arg.

The method of molecular modeling studies on the (S)-3/D- and L-Arg

Conducted further molecular modeling studies on the (S)-**3**/D- and L-Arg by using the Gaussian with the density functional theory (DFT) method at the B3LYP level.